49. B. V. Derjaguin, N. V. Churaev, and V. M. Muller, Surface Forces, Consultants Bureau, New York, 1987.
50. P. G. de Gennes, Modern Phys. 57(3):827–863 (1985).

3
Shape of Meniscus/Film Transition Region

GEORGE J. HIRASAKI Shell Development Company, Bellaire Research Center, Houston, Texas

Summary 77
I. Introduction 78
II. Analysis 79
A. Assumptions 79
B. Integration of the augmented Laplace-Young equation 80
C. Extrapolation to zero thickness 83
III. Interpretation of Profiles 84
IV. Contact-Angle Hysteresis 89
V. Numerical Integration of Profiles 90
VI. Calculated Profiles 91
A. Changing electrostatic interactions 91
B. Changing van der Waals interactions 91
C. Changing structural interactions 92
VII. Conclusions 94
Symbols 96
References 98

SUMMARY

The equilibrium shape of the meniscus/film transition region can be determined from the disjoining pressure isotherm, the value of the capillary pressure, and the augmented Laplace–Young equation. The contact angle is determined by a linear extrapolation of the cosine of the angle of inclination of the meniscus to zero thickness.

This method illustrates how the disjoining pressure isotherm affects the contact angle. The condition for hysteresis in the equilibrium contact angle on a smooth, homogeneous substrate is identified.

I. INTRODUCTION

The surface forces in the transition region between the meniscus and the thin, uniform film determine the contact angle. The contact angle can be expressed as a function of an integral of the disjoining pressure isotherm between the limits of the thickness of the film and the essentially infinite thickness in the meniscus. Whether the state of wetting is complete or incomplete can be determined from the sign of the integral (see Chapter 2).

The augmented Laplace–Young equation and the disjoining pressure isotherm can be used to determine the shape of the interfacial profile in the transition region. The approach used here is the same as that introduced by Martynov et al. [1], except for the choice of boundary conditions. Their system was a meniscus in a slot of given width. Deryagin et al. [2] have derived analytical expressions for the profile of the transition region between a meniscus and a wetting film (see Fig. 1) by using a simple model for the disjoining pressure. Renk, Wayner, and Homsy [3] derived a solution for the profile of the transition region using the method of matched asymptotic expansions. They used a disjoining pressure with an inverse third power dependence on the film thickness. Truong and Wayner [4] measured the shape of the meniscus and transition region using interferometry and the thickness of the wetting film (see Figs. 1 and 8) using ellipsometry and compared the observations with theory. They observed the length of the transition region for this wetting system to be about 20 μm. Adamson and Zebib [5] have used a numerical shooting method to calculate the transition between a vertical film and the meniscus connecting to a horizontal liquid surface. They considered only wetting films with van der Waals or BET isotherms. Zorin, Platikanov, and Kolarov [6] measured the thickness of the uniform film, the transition region, and the meniscus (see Figs. 1 and 8) of water or electrolyte solutions on quartz by using interferometry. In the case of water, the thickness of the uniform film was 145 nm, while the extrapolated meniscus approached only within 207 nm of the quartz surface. The length of the transition region was about 9 μm. Wayner [7] calculated the profile of the transition region for nonwetting systems (Fig. 1). Starting with zero slope at the thin film, the profile had a substantial curvature as the profile changed to the constant slope of the meniscus. This resulted in a very short transition region. Mohanty [8] has catalogued, as a function of the shape of the disjoining pressure isotherm, the regions of uniform film thickness and nonzero contact angle (first introduced by Dzyaloshinskii, Lifshitz, and Potaevskii [18]).

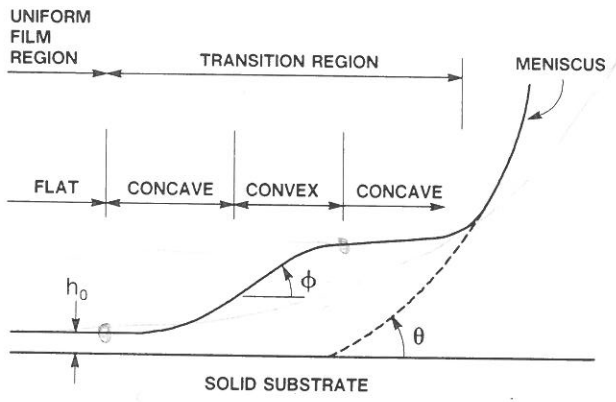

FIG. 1 Profile of film/meniscus transition region.

Here we only discuss systems in which the curvature of the contact line and thus the line tension can be neglected. When this cannot be neglected, a more detailed analysis is needed to determine the line tension [9–14].

The profile of the transition region has been determined only for continuous profiles. Recognizing that a discontinuity can exist with some conditions, Chuarev, Starov, and Derjaguin [4] derived the sufficient conditions for a continuous profile.

Hysteresis of the contact angle is usually attributed to nonequilibrium effects, contamination, or heterogeneity of the surface due to either roughness or composition [5]. Martynov et al. [1] described the hysteresis that can occur as a result of lack of attainment of hydrodynamic equilibrium between the transition region and the uniform film region. It will be shown here that hysteresis is possible on a homogeneous surface in local equilibrium when a metastable film state exists.

The contact angle is usually determined experimentally by extrapolating the shape of the meniscus profile to zero thickness. It will be shown here that the profile of the cosine of the angle of inclination of the interface in the meniscus region versus thickness is a straight line in the absence of gravity and the linear extrapolation to zero thickness will give the contact angle.

II. ANALYSIS

A. Assumptions

The system that is considered here is the three-phase contact region between two fluids and a homogeneous, flat solid. The equations derived here will transform to that for a symmetrical film (identical bulk phases) by multiplying the interfacial tension by a factor of two. The system is in chemical equilibrium. Gravity is not considered.

It is assumed that the curvature of the contact line is small compared to that of the meniscus so that the system can be modeled as translationally invariant (i.e., straight contact line and only one finite principle radius of curvature). The mean curvature of the interface can then be described by the curvature of a curve.

It is assumed that the interfacial tension between the two fluids is a constant equal to the value between bulk phases. It is recognized that the sum of the two interfacial tensions is not constant when the disjoining pressure is nonzero, but there is no means of determining one interfacial tension independent of the other. The sensitivity of the result to the assumption of constant interfacial tension can be estimated by assuming that the interfacial tension changes by an amount equal to the spreading coefficient.

It is assumed that the radius of curvature of the interface is large compared to the range of the surface forces. This assumption will allow the disjoining pressure to be expressed as a function of the film thickness alone and independent of the slope and curvature. In the following, a case will be considered where the assumption is violated.

B. Integration of the Augmented Laplace–Young Equation

A diagram of the meniscus/film transition region is shown in Fig. 1. The film region is flat with an equilibrium film thickness h_0. The inclination of the interface is given by the angle ϕ. The meniscus has a constant curvature. Extrapolation of the profile of the meniscus with a constant curvature to the surface of the solid substrate gives the contact angle θ.

A necessary condition for equilibrium is the augmented Laplace–Young equation (see Chapter 2). This necessary condition can be determined by either the local minimization of energy or the minimization of the energy functional over the entire profile by application of the calculus of variations:

$$P_c = \Pi + 2H\gamma \tag{1}$$

where P_c is the capillary pressure defined as the pressure of the bulk fluid phase minus the pressure of the film phase. It is constant throughout the system because there is no gravitational field and the system is in equilibrium. The term Π is the disjoining pressure, H is the mean curvature of the interface, and γ is the interfacial tension, which is assumed to be a constant equal to the value between the bulk phases.

Since the system is assumed to be translationally symmetric, twice the mean curvature is equal to the curvature of the interfacial profile. The curvature of the profile is equal to the rate of change of the angle of inclination with respect to the arc length s:

$$2H = \frac{d\phi}{ds} \tag{2}$$

Trigonometric relations can be used to express the curvature in terms of the derivative of the cosine of the angle of inclination with respect to the film thickness:

$$\frac{d\phi}{ds} = \frac{dh}{ds}\frac{d\phi}{dh} \tag{3a}$$

$$= \sin\phi \frac{d\phi}{dh} \tag{3b}$$

$$= -\frac{d\cos\phi}{dh} \tag{3c}$$

The augmented Laplace–Young equation can now be expressed as a first-order differential equation:

$$-\gamma d\cos\phi = (P_c - \Pi)\, dh \tag{4a}$$

$$= d\psi \tag{4b}$$

The function $\psi(h)$ is similar to the specific interaction potential [1] except that P_c is the parameter rather than Π_{eq}. On a flat substrate they are equal. It should also be noted that this function has the opposite sign compared to the ψ function of Martynov et al. [1]. Equation (4) is integrated with the lower limit of the integration taken to be the uniform film thickness where the angle of inclination is zero and ψ is defined to be equal to zero:

$$1 - \cos\phi(h) = \gamma^{-1}\psi(h) \tag{5}$$

where

$$\psi(h) = \int_{h_0}^{h} (P_c - \Pi)\, dh \tag{6}$$

The function $(1.0 - \cos\phi)$ is similar to the function K(h) introduced by Mohanty (p. C-60) [8].

The disjoining pressure isotherm and the corresponding graph of $1.0 - \cos\phi(h)$ are shown in Fig. 2. The graph of the function ψ is the same as that for the specific interaction potential, since the equilibrium disjoining pressure of the flat, equilibrium film is equal to the capillary pressure. In particular, the local minima correspond to local equilibrium states of flat films. The zeros of the function

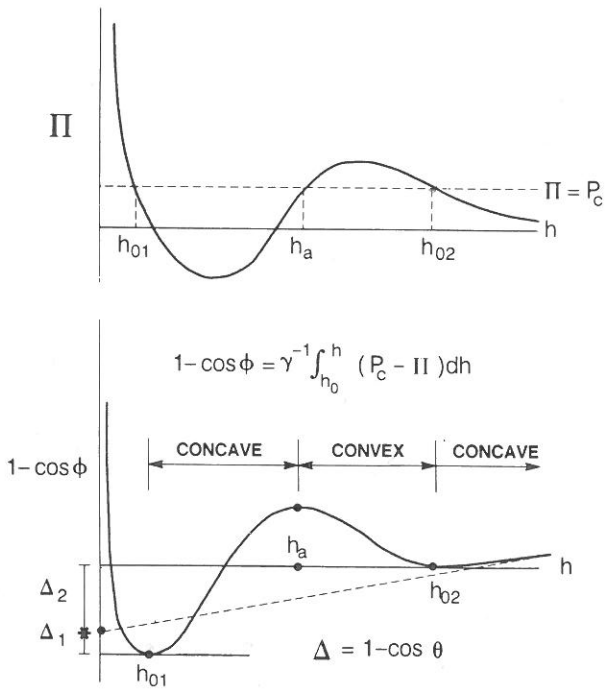

FIG. 2 Disjoining pressure isotherm and angle of inclination.

occur at either h_{01} or h_{02}, depending on which locally stable state corresponds to the state of the uniform film. It is obvious that for a uniform film in equilibrium with a meniscus, a locally stable film state cannot have another locally stable state with a greater thickness that has a lower minimum, since this would result in non-existent values of the inclination angle. However, there is no restriction on another locally stable state with a smaller thickness that has a lower minimum, since the transition region will not pass through the smaller thickness.

The curve of $1.0 - \cos\phi$ has its extrema at the thicknesses where the disjoining pressure isotherm intersects the line $\Pi = P_c$. The extremum is a minimum if the disjoining pressure isotherm has a negative slope at the intersection. The interfacial profile is concave ($2H > 0$) in the regions where the curve of $1.0 - \cos\phi$ has a positive slope and is convex ($2H < 0$) where it has a negative slope (see Figs. 1 and 2). From Eq. (6), it can be seen that the profile

is concave when the disjoining pressure isotherm is below the line $\Pi = P_c$ and is convex when above the line [1].

C. Extrapolation to Zero Thickness

The contact angle is defined as the angle that the extrapolated meniscus profile makes with the solid substrate. The meniscus is the portion of the profile where the disjoining pressure is essentially zero. Thus Eq. (1) shows that the meniscus profile will have a constant curvature and Eq. (6) shows that the slope of $\psi(h)$ is equal to P_c. Let h_* be a thickness in the meniscus region from where the profile is to be extrapolated. Extrapolation of the $\psi(h)$ curve from this straight line portion of the curve can be expressed as

$$\psi_*(0) = \psi(h_*) + \frac{d\psi}{dh}(h_*)(0 - h_*) \tag{7}$$

Using the additional relation

$$\Pi(h \geq h_*) = 0 \tag{8a}$$

$$\Pi(h_0) = P_c \tag{8b}$$

$$\frac{d\psi}{dh}(h_*) = P_c \tag{8c}$$

$$\psi(h_*) = \int_{h_0}^{h_*} (P_c - \Pi)\, dh \tag{8d}$$

and by integration by parts, the extrapolated value of ψ is

$$\psi_*(0) = -\int_0^{\Pi(h_0)} h\, d\Pi \tag{9a}$$

$$= - S^{eq}_{\sigma/\alpha\beta} \tag{9b}$$

where $S^{eq}_{\sigma/\alpha\beta}$ is the equilibrium spreading coefficient (see Chapter 2). From Eq. (5) and the definition of the contact angle, the angle of the extrapolated profile is

$$\cos\theta = 1 + \frac{\int_0^{\Pi(h_0)} h\, d\Pi}{\gamma} \tag{10a}$$

$$= 1 + \frac{S^{eq}_{\sigma/\alpha\beta}}{\gamma} \qquad (10b)$$

This expression is the Young equation expressed in terms of the spreading coefficient (see Chapter 2).

The extrapolation of the profile from the meniscus is illustrated on Fig. 2 by the dashed line. The origin of the ordinate depends on whether the film thickness is at h_{01} or h_{02}. The extrapolated value of $1.0 - \cos\phi$ that is equal to $1.0 - \cos\theta$ is denoted by Δ. If the film thickness is h_{01}, then Δ is positive and a finite contact angle exists. If the film thickness is h_{02}, then Δ is negative and a finite contact angles does not exist. In this case the extrapolated profile becomes parallel to the substrate surface at a thickness corresponding to where the extrapolated profile intersects the axis of $1.0 - \cos\phi = 0$. Thus the film is completely wetting in the latter case.

III. INTERPRETATION OF PROFILES

The preceding analysis will be used to interpret the interfacial profiles as a function of the disjoining pressure isotherm and the value of the capillary pressure. Equation (4a) shows that the extrema of $\cos\phi$ occur at thickness where the disjoining pressure pressure isotherm intersects the line $\Pi = P_c$. The profile is convex for thicknesses where the disjoining pressure isotherm is above the line $\Pi = P_c$ and is concave below the line [1]; see Fig. 2.

Uniform (flat) films can exist where the disjoining pressure isotherm intersects the line $\Pi = P_c$ and has negative slope at the intersection. Figure 2 shows two such intersections where uniform equilibrium films can exist. Since the shape of the curves of $1.0 - \cos\phi$ is the same as for the specific interaction potential with constant equilibrium disjoining pressure, both thicknesses are local equilibrium thicknesses for uniform films, and the thickness with the lower value of $1.0 - \cos\phi$ is the more stable thickness. If the smaller thickness, h_{01}, is more stable, then it is possible for the uniform film to have its thickness equal to either h_{01} or the metastable thickness, h_{02}. However, if the larger thickness, h_{02}, is more stable, then the only uniform film in equilibrium with the meniscus is h_{02}. This can be proven with a graph of $1.0 - \cos\phi$ because if the uniform film had as its thickness the less stable thickness, h_{01}, the values of $1.0 - \cos\phi$ in the neighborhood of h_{02} would be less than zero, an impossible situation. If the two thicknesses are equally stable, then the uniform film can be either h_{01} or h_{02} and the contact angle with either uniform film is the same.

Figure 3 shows the effect of capillary pressure on the interfacial profile. The equilibrium thickness of the flat film is a function

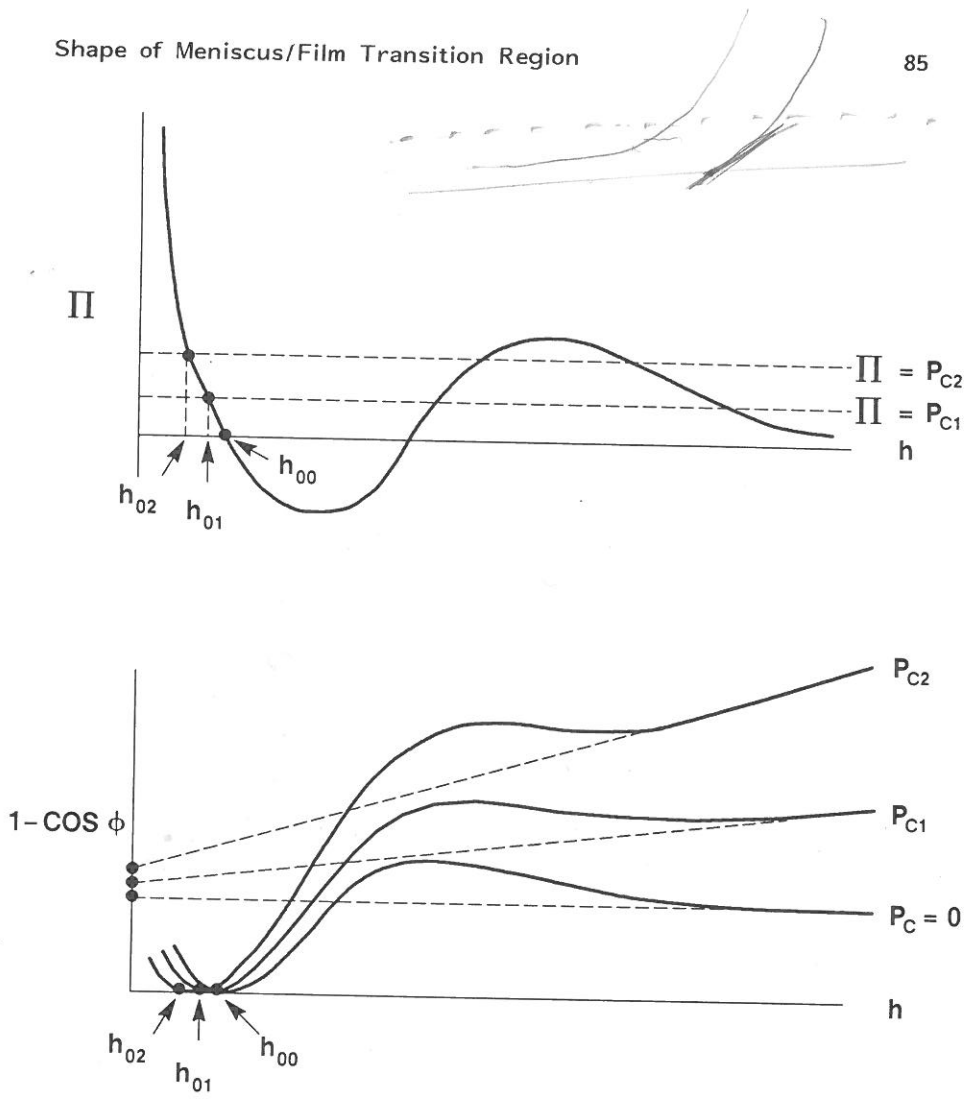

FIG. 3 Effect of capillary pressure on interfacial profile.

of the capillary pressure. The curves of $1.0 - \cos\phi$ have different limiting slopes in the meniscus region equal to the capillary pressure divided by the interfacial tension. Because the uniform film thicknesses and equilibrium disjoining pressure are different, the intersection of the extrapolated profile with the substrate and thus the contact angle is different.

A case with only repulsion is shown in Fig. 4. In this case the profile becomes parallel with the substrate at h_p and the extrapolated profile does not intersect the substrate.

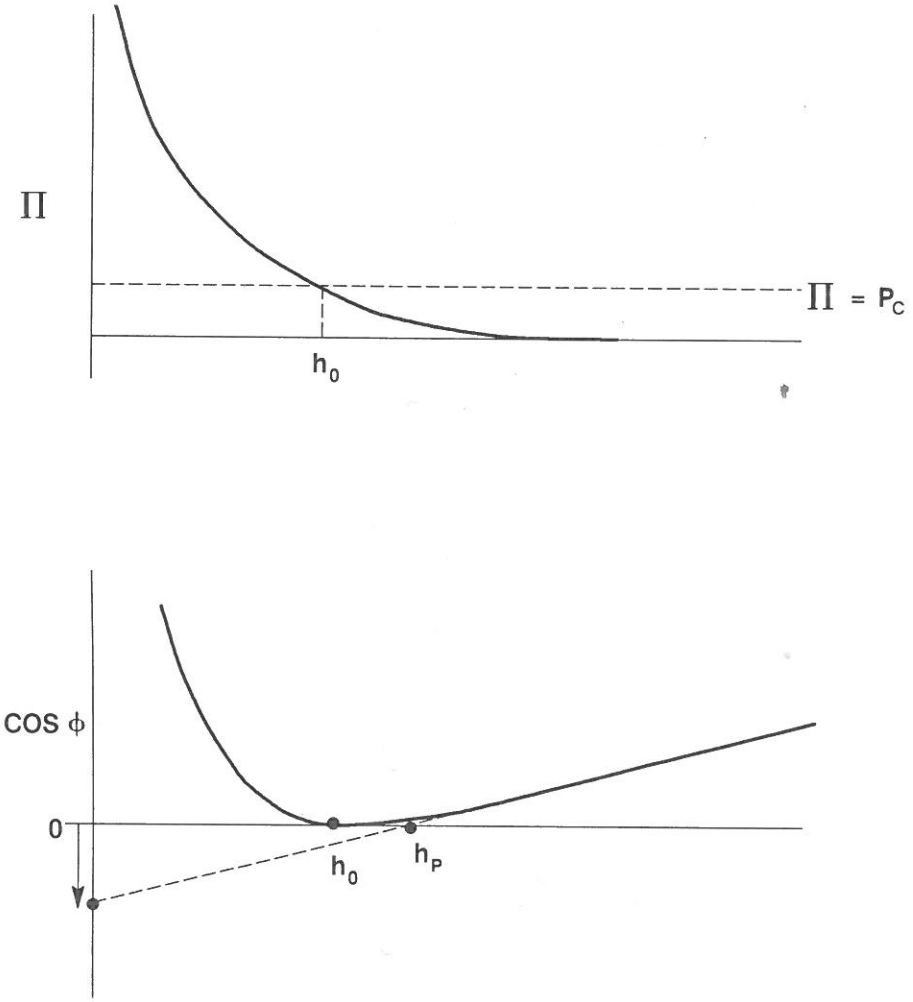

FIG. 4 Disjoining pressure with repulsion only.

A case with long-range attraction and only short-range repulsion is shown in Figure 5. The profile is concave and the extrapolated profile intersects the substrate at a finite contact angle. If the disjoining pressure isotherm on Fig. 2 has a long-range attraction, then the curve of 1.0 − cos ϕ will approach the extrapolated line from below as in Fig. 5.

A case with net attraction at medium thicknesses and net repulsion at large thicknesses is illustrated on Fig. 6. In the case

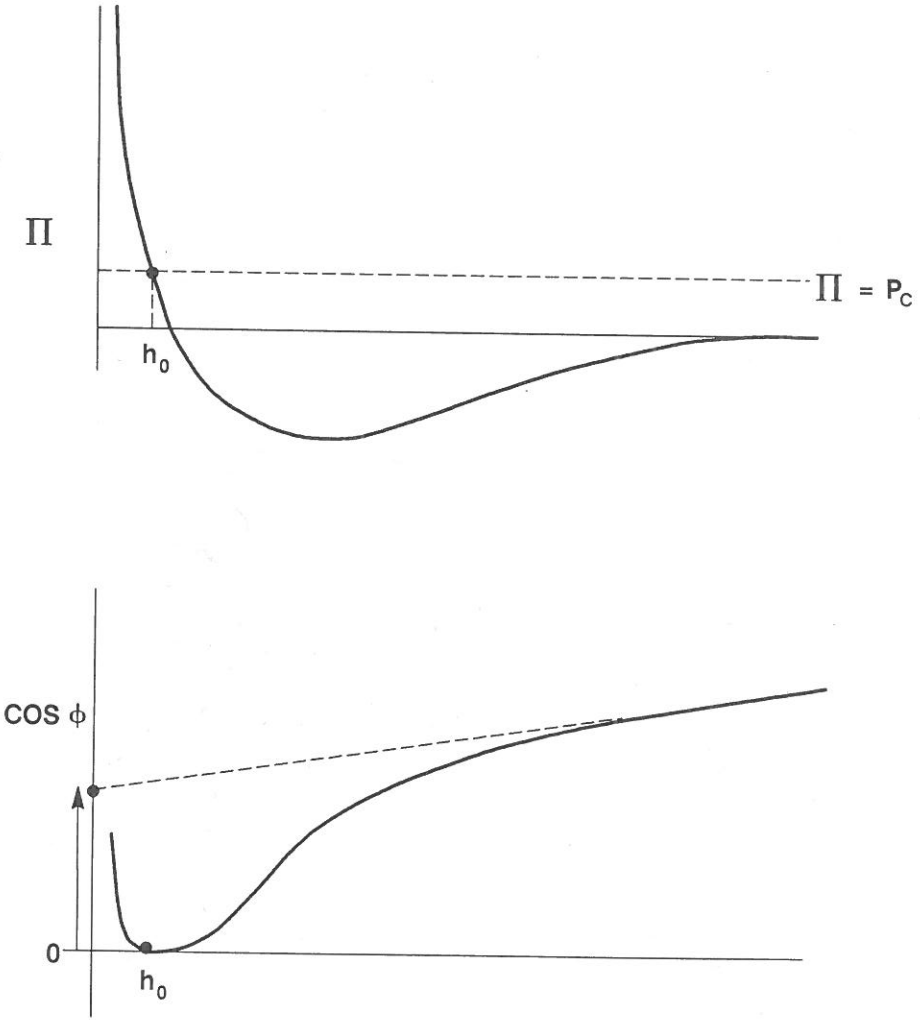

FIG. 5 Disjoining pressure with long-range attraction and short-range repulsion.

illustrated, the capillary pressure and/or net attraction is large enough such that the value of 1.0 − cos ϕ exceeds 1.0 for an interval. Such an interval will not exist in reality. As the profile approaches vertical, the curvature becomes large and the disjoining pressure will become a function of curvature or slope. This limiting case was pointed out by Martynov et al. [1].

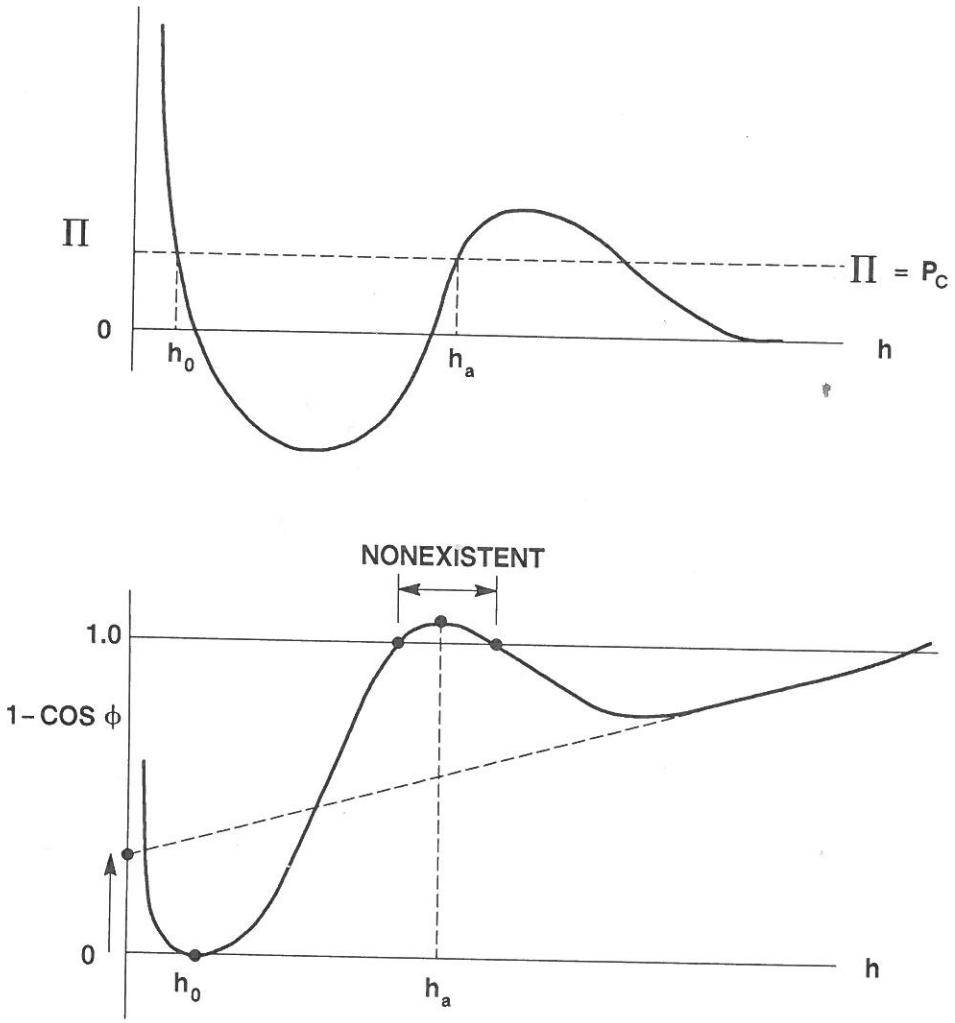

FIG. 6 Discontinuous profile.

Figure 6 illustrates a sufficient condition for a discontinuity in the film thickness in the transition region, but this is not a necessary condition for a discontinuity. A discontinuity in thickness could conceivably exist with finite slope on either side of the discontinuity. For example, it is known that flat films are not stable in the range of thicknesses where the disjoining pressure isotherm has a positive slope. Churaev, Starov, and Derjaguin [4], using the

Jacobi's condition of calculus of variations, derived the sufficient condition for a continuous profile. They show that, when the length of transition region is less than a critical length determined by the maximum positive slope of the disjoining pressure isotherm, the profile of the transition region is continuous. They conclude that the smallness of the contact angle is a sufficient condition for the existence of gently sloping stable profiles of the transition region, even though the disjoining pressure isotherm may have a positive slope.

IV. CONTACT-ANGLE HYSTERESIS

Metastable film states are possible when the disjoining pressure isotherm has multiple thicknesses with the same value of the disjoining pressure. It was pointed out earlier that for metastable uniform film states in equilibrium with a meniscus to exit, it is necessary for the smaller of the two possible local equilibrium thicknesses to be the more stable thickness. This is the case illustrated in Fig. 2. Since only equilibrium phenomena are considered here, differences between advancing and receding contact angles will only be attributed to different locally stable states of the uniform film. If a meniscus advances on a uniform film corresponding to h_{01}, then a finite contact angle will result. However, if the uniform film resulted from thinning the bulk fluid with a receding meniscus in such a manner that the thickness remained at the metastable thickness, h_{02}, then there will be no finite contact angle.

Zorin and Churaev [6] describes an experiment with water films on quartz where metastable films were observed. The uniform film with a thickness of about 10 nm that existed after a bubble was pressed against a quartz plate for 10–to–15 h had a finite contact angle with the meniscus. When the meniscus was receded, a uniform, wetting film with a thickness of about 40 nm was left behind. There was a sharp boundary between the two films that did not change its appearance for several hours. Condensation of water on these films resulted in dew drops on the thinner film and the boundary between the films but not on the thicker, wetting film.

Zorin and Churaev [6] claim that the two films coexist. The observation of different contact angles for the two films and the earlier analysis of the contact angle of metastable film states suggest that these two films do not have the same value of the interaction potential and thus will not coexist at equilibrium. In addition to metastable states, contact-angle hysteresis can occur due to the dependence of the contact angle on the capillary pressure discussed earlier.

V. NUMERICAL INTEGRATION OF PROFILES

The profiles of the transition region were calculated from numerical integration of Eq. (4) and trigonometric definitions:

$$\frac{d(1 - \cos \phi)}{dh} = (P_c - \Pi(h))/\gamma \tag{11}$$

From trigonometric relations the differential of the distance along the plane of the solid can be expressed as a function of the angle:

$$\frac{dx}{dh} = \frac{1}{(1/\cos^2 \phi - 1)^{1/2}} \tag{12}$$

Equations (11) and (12) are a system of two first-order ordinary differential equations that can be integrated from some initial condition using a method such as the fourth-order Runge–Kutta method. The equilibrium film thickness h_0 on the solid is determined using the Newton method to search for the thickness at which the disjoining pressure is equal to the capillary pressure. This search is limited to within a specified range because of possible multiple roots. The initial condition for the integration is determined by making a small perturbation in the thickness from the equilibrium film thickness and estimating the value of $1 - \cos \phi$ by evaluating the right-hand side of Eq. (11) at one-half of the perturbed thickness value. Equations (11) and (12) are numerically integrated until $1 - \cos \phi$ is equal to 10^{-5}. The profile at this point is specified for plotting purposes to be the origin of the distance scale along the plane of the solid. The profile is numerically integrated using Eqs. (11) and (12) to a thickness of 100 nm, a thickness at which the disjoining pressure is usually negligible. The disjoining pressure is then turned off, and the "extrapolated meniscus profile" is integrated to smaller thicknesses until the profile either intersects the solid or becomes parallel with the plane of the solid. When the profile intersects the solid, the angle at intersection is the macroscopic contact angle θ. This numerically determined contact angle compares well with the theoretical value calculated from the following equation (see Chapter 2):

$$1 - \cos \theta = \frac{1}{\gamma} \int_0^{\Pi(h_0)} h \, d\Pi = \frac{1}{\gamma} \left(P_c h_0 + \int_{h_0}^{\infty} \Pi \, dh\right) \tag{13}$$

VI. CALCULATED PROFILES

The following examples have disjoining pressure isotherms that are perturbations from the base case of SPE/DOE 17367 [18]. The base case parameters are given in Table 1. All cases have a capillary pressure of 10 kPa (1.4 psi).

The expression for the electrostatic interaction is given in reference 17. Here the electrical potentials of the two surfaces will always be specified to be equal, resulting in a repulsive interaction. The van der Waals interaction is calculated from the following expression:

$$\Pi_{vdW} = -\frac{A}{6\pi h^3} \tag{14}$$

where A is the Hamaker constant. The structural interaction is calculated from the following expression:

$$\Pi_s = A_s e^{-h/h_s} \tag{15}$$

where A_s is the coefficient and h_s is the characteristic decay length for the exponential model.

A. Changing Electrostatic Interactions

Disjoining pressure isotherms with changing repulsion are illustrated on Fig. 7. The van der Waals contribution is turned off, and the electrostatic contribution is increased by increasing the electrical potential from 0 to 10, 30, and 60 mV. When there is no electrostatic contribution, the only contribution is the repulsive structural contribution. The profiles are illustrated on Fig. 8. An open symbol marks the equilibrium film thickness. The profiles for the case with zero potential overlap because, as Fig. 7 shows, the disjoining presure goes to zero after a small increase above the equilibrium film thickness. With increased electrical potential, the equilibrium film thickness increases and the profile increases in slope more gradually. In all cases the profiles with the disjoining pressure turned off (the extrapolated meniscus profile) becomes tangent to the plane of the solid surface, and thus the contact angles are zero.

B. Changing van der Waals Interactions

Figures 9 and 10 show the disjoining pressure isotherms and profiles for the case of electrostatic contribution turned off and the Hamaker constant increased from 0 to 3×10^{-20} J. The range of the forces

Isotherms With Changing Electrostatic Interactions
van der Waals Turned Off

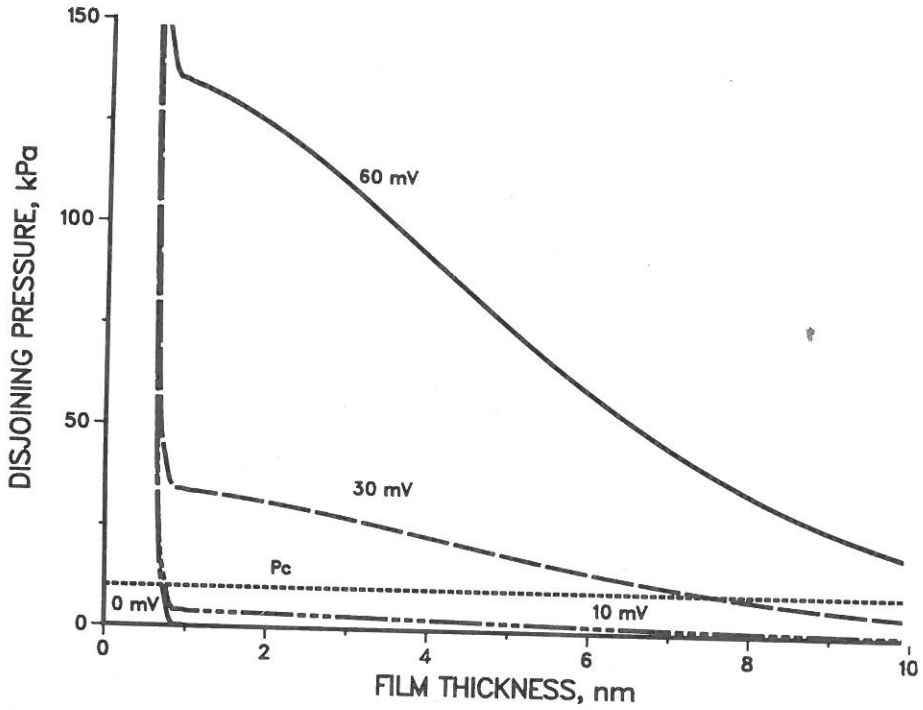

FIG. 7 Repulsive disjoining pressure isotherms.

are now much shorter and are negative or attractive. Increasing the Hamaker constant decreases the equilibrium film thickness and increases the contact angle.

C. Changing Structural Interactions

The change in the disjoining pressure isotherm resulting from perturbations in the structural forces from the base case is shown in Fig. 11. The changes affected the "cut-off distance" at which the attractive van der Waals forces became dominated by the short-range repulsive structural forces. The effect on the interaction potentials is shown in Fig. 12. The "cut-off distance" determines how low the interaction potential becomes before it is "cut off" by the short-range repulsion. The contact angle is determined by the value of the minimum of the interaction potential. The profiles of the interfaces are shown in Fig. 13. Decreasing the cut-off distance decreases the equilibrium film thickness and increases the contact angle.

Interface Shape With Changing Electrostatic Interactions
van der Waals Turned Off

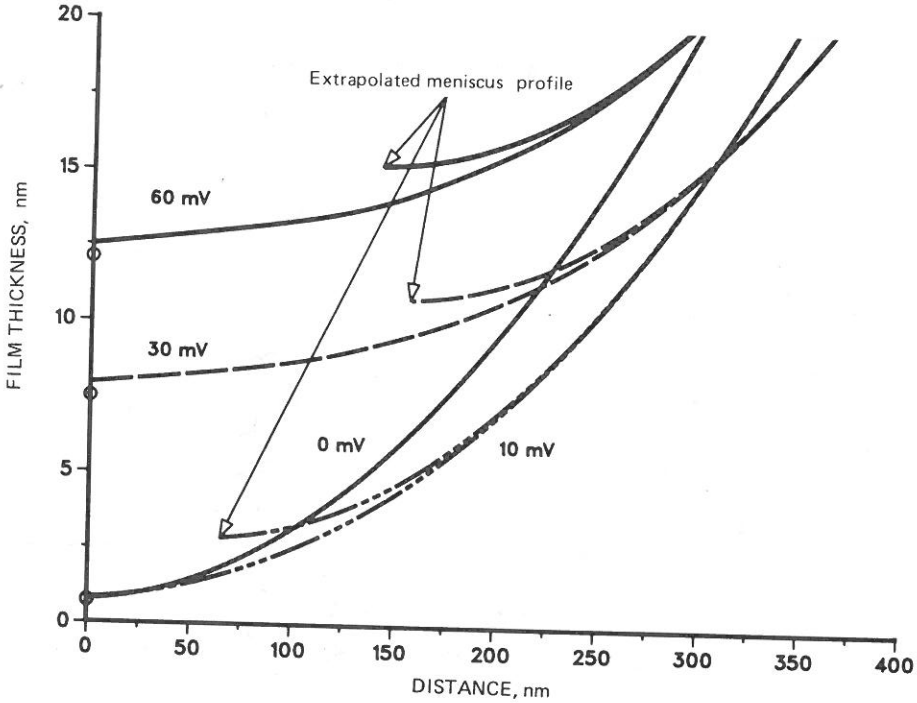

FIG. 8 Interfacial profiles with repulsive disjoining pressures and positive capillary pressures.

TABLE 1 Model Parameters for Base Case

Hamaker constant	1×10^{-20} J
Electrolyte concentration	0.01 M
Surface electrical potentials	−60. mV
Coefficient for structural force	1.5×10^{7} kPa
Decay length for structural force	0.05 nm
Interfacial tension	25 mN m^{-1}
Capillary pressure	10 kPa

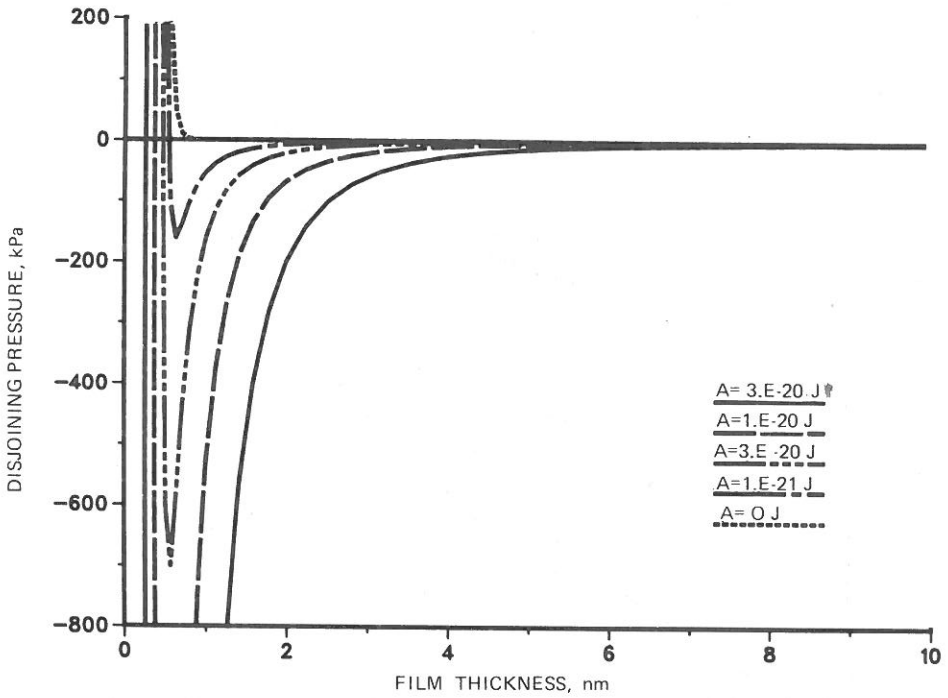

FIG. 9 Disjoining pressure isotherms with different van der Waals interactions.

VII. CONCLUSIONS

1. The profile of the transition region between the uniform film and the meniscus can be determined from the disjoining pressure isotherm, capillary pressure, and the solution of the augmented Laplace—Young equation.
2. By expressing the profile as a graph of $1.0 - \cos \phi$ versus thickness, the curve has the same shape as that for the specific interaction potential and the stability of the uniform film regions can be interpreted from the relative values of the specific interaction potential. Also, the meniscus region is a straight line with a slope equal to the capillary pressure divided by the interfacial tension. The contact angle is determined by extrapolating the straight line to zero thickness.
3. Contact-angle hysteresis on a homogeneous substrate with the system at equilibrium can result from metastable uniform films.

Interface Shape With Changing van der Waals Interactions
Electrostatics Turned Off

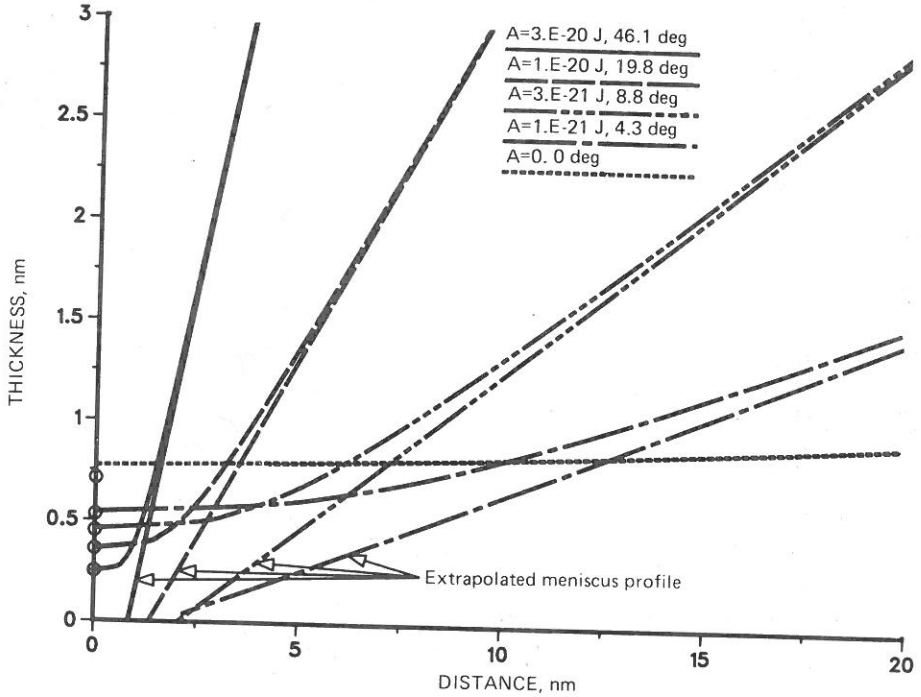

FIG. 10 Interfacial profiles with short-range repulsion and longer-range attractive disjoining pressure isotherms.

4. When the disjoining pressure isotherm is strictly repulsive, the meniscus profile calculated back to the solid with the disjoining pressure turned off (extrapolated meniscus profile) does not intersect the solid but rather becomes tangent to the plane of the solid. The contact angle is zero.
5. When the disjoining pressure has short-range repulsion and long-range attraction, the meniscus profile calculated back to the solid with the disjoining pressure turned off intersects the solid. The contact angle is nonzero.
6. Small changes in the range of the structural forces greatly affect the minimum in the interaction potential and the contact angle.

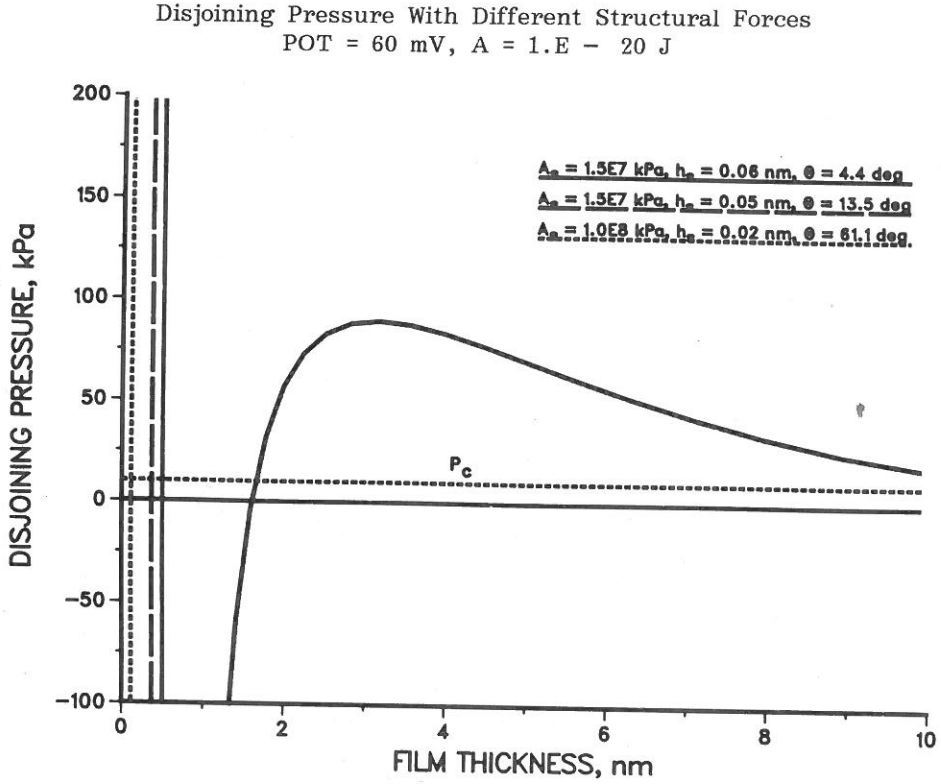

FIG. 11 Disjoining pressure isotherms with different range of structural forces.

SYMBOLS

A_S	structural component coefficient, Pa
A	Hamaker constant, J
h	thickness, m
H	mean curvature, m^{-1}
P_C	capillary pressure, Pa
s	arc length, m
$S^{eq}_{\sigma/\alpha\beta}$	equilibrium spreading coefficient, J m^{-2}

Greek Letters

ϕ	angle of inclination
γ	interfacial tension, J m^{-2}

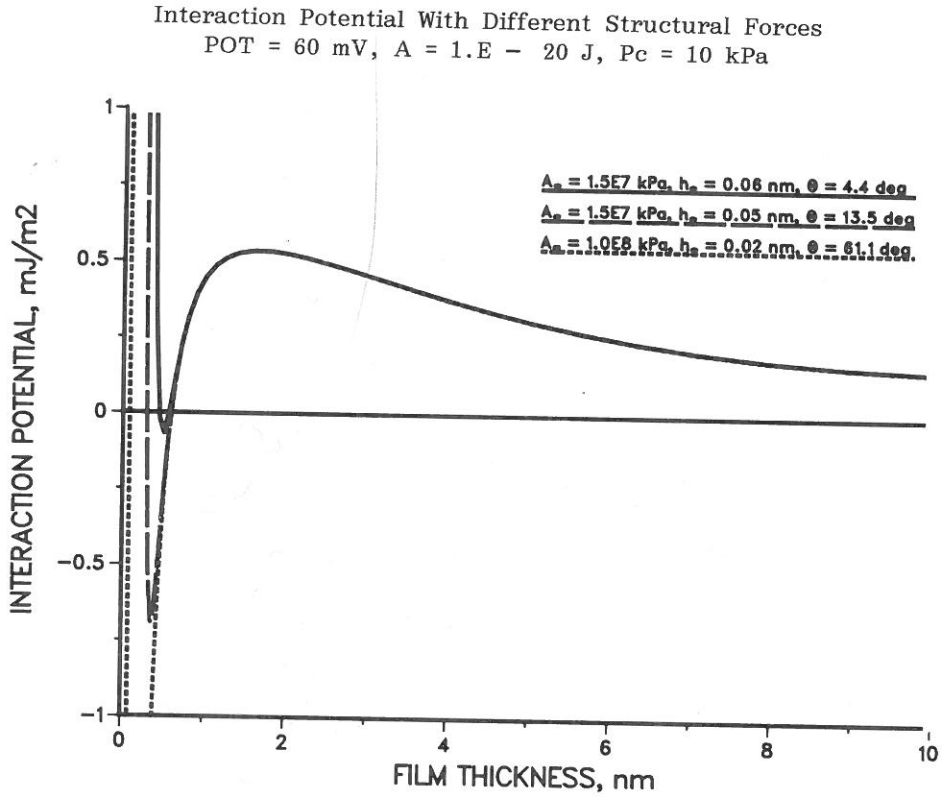

FIG. 12 Interaction potentials with different range of structural forces.

Π	disjoining pressure, Pa
ψ	function of thickness, J m^{-2}
θ	contact angle
Δ	1.0 − cos θ

Subscripts

o	uniform film
*	meniscus region
p	where extrapolated profile becomes parallel to substrate
s	structural component
vdW	van der Waals component

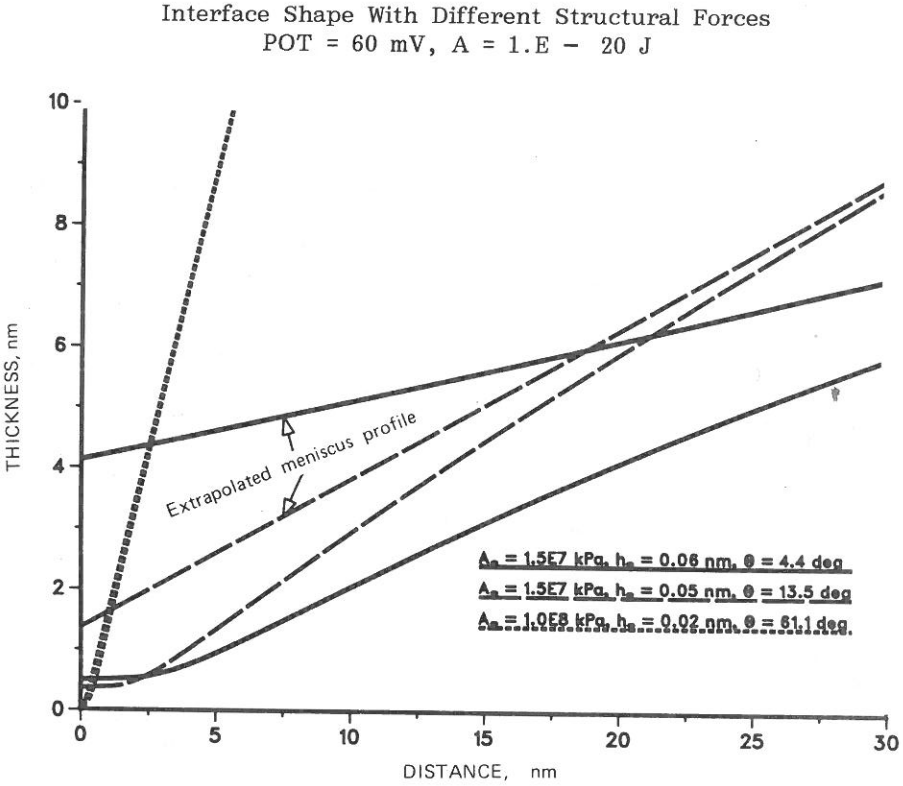

FIG. 13 Interfacial profiles with different range of structural forces.

REFERENCES

1. G. A. Martynov, V. M. Starov, and N. V. Churaev, Colloid J. (U.S.S.R.) 39:406–417 (1977).
2. B. V. Deryagin, V. M. Starov, and N. V. Churaev, Colloid J. (U.S.S.R.) 38:786–789 (1976).
3. F. Renk, P. C. Wayner, and G. H. Homsy, J. Colloid Interface Sci. 67:408–414 (1978).
4. J. C. Troung and P. C. Wayner, Jr., J. Chem. Phys. 87(7): 4180–4188 (1987).
5. A. W. Adamson and A. Zebib, J. Chem. Phys. 84:2619–2623 (1980).
6. Z. Zorin, D. Platikanov, and T. Kolarov, Colloids Surfaces 22: 147–159 (1987).
7. P. C. Wayner, Jr., J. Colloid Interface Sci. 77(2):495–500 (1980).

8. K. K. Mohanty, Fluids in Porous Media: Two-Phase Distribution and Flow, Ph.D. thesis, University of Minnesota, Minneapolis, 1981.
9. J. A. de Feijter and A. Vrij, J. Electroanal. Chem. 37:9–22 (1972).
10. P. A. Kralchevsky and I. B. Ivanov, Chem. Phys. Lett. 121(1,2):111–115 (1985).
11. P. A. Kralchevsky and I. B. Ivanov, Chem. Phys. Lett. 121(1,2):116–120 (1985).
12. V. G. Babak, Colloids Surfaces 25:1–24 (1987).
13. V. G. Babak, Colloids Surfaces 25:25–39 (1987).
14. N. V. Churaev, V. M. Starov, and B. V. Derjaguin, J. Colloid Interface Sci. 89(1):16–24 (1982).
15. A. W. Adamson, Physical Chemistry of Surfaces, 3rd ed., John Wiley & Sons, New York, 1976, pp. 339–357.
16. Z. M. Zorin and N. V. Churaev, Colloid J. (U.S.S.R.) 30:279–281 (1968).
17. G. J. Hirasaki, Wettability: Fundamentals and Surface Forces, SPE/DOE 17367, paper prepared for the 1988 SPE/DOE Symposium on Enhanced Oil Recovery, Tulsa, Okla., 1988.
18. I. E. Dzyaloshinskii, E. M. Lifshitz, and L. P. Pitaevskii, Adv. Phys. 10:165–209 (1961).